

A galaxy as the source of a C IV absorption system close to the epoch of reionization^{*}

C. Gonzalo Díaz^{1†}, Emma V. Ryan-Weber¹, Jeff Cooke¹, Max Pettini^{2,3}
and Piero Madau⁴

¹Centre for Astrophysics & Supercomputing, Swinburne University of Technology, Mail H39, PO Box 218, Hawthorn, 3122 VIC, Australia

²Institute of Astronomy, Madingley Road, Cambridge, CB3 0HA

³Kavli Institute for Cosmology, Madingley Road, Cambridge, CB3 0HA

⁴Department of Astronomy & Astrophysics, University of California, Santa Cruz, CA 95064, USA

Accepted. Received

ABSTRACT

We find a bright ($L_{UV} = 2.5 L_{z=6}^*$) Lyman alpha emitter (LAE) at redshift $z = 5.719$ at a projected distance of 79 physical kpc from a strong triply ionized carbon (C IV) absorption system at redshift $z = 5.7238$ previously reported in the spectrum of the $z_{em} = 6.309$ QSO SDSS J1030+0524. This is the highest redshift galaxy-absorber pair detected to-date, supporting the idea that galaxy-wide outflows were already in place at the end of the epoch of reionization. The proximity of this object makes it the most likely source of metals, consistent with models of outflows at lower redshift where significant observational evidence relates metal absorption systems with galaxies hosting outflows.

In a typical outflow scenario, a wind of 200 km s^{-1} , active since the universe was only 0.6 Gyr old ($z \sim 8.4$), could eject metals out to 79 kpc at $z = 5.719$. Although the origin of metals in the intergalactic medium (IGM) is still under debate, our results are consistent with predictions from cosmological simulations which reproduce the evolution of the cosmic density of C IV from $z \sim 6$ to the present day based on outflow-driven enrichment of the IGM.

We also report two more Ly α emitters in this field, at $z = 5.973 \pm 0.002$ and $z = 5.676 \pm 0.002$ respectively, the former confirming the original identification by Stiavelli et al. Our results suggest that the colour cut typically used to identify *i*-dropouts ($i_{775} - z_{850} > 1.3$) misses a non-negligible fraction of blue galaxies with faint UV continuum at $z \gtrsim 5.7$.

Key words: early universe, galaxies: high redshift, galaxies: intergalactic medium, galaxies: distances and redshifts.

1 INTRODUCTION

Medium and high resolution spectroscopy has revealed the presence of metals in the high redshift intergalactic medium (IGM) through the detection of absorption systems in the spectra of background quasi stellar objects (QSOs) (e.g. Songaila 2001; Pettini et al. 2003; Simcoe 2006; Becker et al. 2006; Becker, Rauch & Sargent 2009; Ryan-Weber et al. 2009; Becker et al. 2011; Simcoe et al. 2011). However, the enrichment source of these absorption

systems is still poorly constrained. There is a debate as to whether these intergalactic metals originated in the recent past from nearby galaxies driving large-scale outflows of their interstellar media, or whether the IGM may have received a ‘blanket’ enrichment at much earlier times, when the Universe became reionised by the first stars and galaxies.

Porciani & Madau (2005) favour the “pre-galactic enrichment” scenario, arguing that the cross-correlation function between Lyman break galaxies (LBGs) and C IV absorbers at $z \sim 3$, as well as the mean absorption line density, can be explained by enriched supernova (SN) driven winds from dwarf galaxies at $z > 6$ (Madau, Ferrara & Rees 2001). These LBG progenitors could generate metal bubbles

^{*} Based on observations collected at the European Organisation for Astronomical Research in the Southern Hemisphere, Chile [VLT program 79.A-0377]

[†] E-mail: gdiaz@astro.swin.edu.au

~ 100 kpc (comoving) in size within the same high-density regions of the IGM where LBGs would later form.

On the other hand, the connection between star forming galaxies and metal absorption features is now firmly established at redshifts $1 \lesssim z \lesssim 3$, strongly supporting the idea that galactic outflows, or ‘superwinds’ as they are often referred to, are one of the main sources of metal enrichment of the IGM, at least at these redshifts (Steidel et al. 2010; Simcoe 2011, and references therein). Evidence for such outflows is provided by the nearly universal blueshift of interstellar absorption lines observed against the nuclei of galaxies undergoing vigorous star formation episodes (e.g. Heckman et al. 2000; Pettini et al. 2001; Shapley et al. 2003; Steidel et al. 2010), with the outflowing gas reaching velocities of up to ~ 1000 km s $^{-1}$ relative to systemic (e.g. Pettini et al. 2002; Quider et al. 2009; Dessauges-Zavadsky et al. 2010, and reference therein). In a recent study of galactic outflows at $z \sim 1.4$, Weiner et al. (2009) found that wind velocities increase with mass and star formation rate ($v_{\text{wind}} \propto \text{SFR}^{0.3}$). A similar trend ($v_{\text{wind}} \propto \text{SFR}^{0.35}$) had previously been shown to hold in ultra luminous infrared galaxies (ULIRGs) at redshift $z = 0.042 - 0.16$ by Martin (2005); both Martin (2005) and Rupke, Veilleux & Sanders (2005) found that 70–85% of ULIRGS at low redshifts ($z < 0.5$) drive such energetic outflows.

The common occurrence of outflows in galaxies undergoing bursts of star formation and the obvious importance of this phenomenon for galaxy evolution and the enrichment of the IGM are some of the reasons why superwinds are attracting a great deal of theoretical interest. One of the goals of current theoretical work is to provide a physical explanation for the somewhat puzzling redshift evolution of the comoving density of C IV ions in the IGM, $\Omega_{\text{C IV}}(z)$. Looking back in time, $\Omega_{\text{C IV}}(z)$ appears to be approximately constant during a ~ 3 Gyr interval between $z \simeq 1.5$ and 5, and then drops by a factor of ~ 3.5 over a period of only ~ 300 Myr from $z = 4.7$ to 5.8 (Ryan-Weber et al. 2009; Becker, Rauch & Sargent 2009; Simcoe et al. 2011).

In a series of papers (Oppenheimer & Davé 2006; Davé & Oppenheimer 2007; Oppenheimer & Davé 2008; Oppenheimer, Davé & Finlator 2009), Oppenheimer and collaborators have explored different wind scenarios using cosmological hydrodynamic simulations which explicitly incorporate outflows from starburst galaxies and concluded that momentum-driven winds give the best agreement with the observations. Interestingly, in their simulations the outflows travel to similar distances $R_{\text{turn}} = 80 \pm 20$ physical kpc at all redshifts they considered. If this is the case in reality, it would imply that at early epochs the metal enrichment by star-forming galaxies affects larger volumes of the Universe than at later times. Tescari et al. (2010) have also highlighted the importance of feedback from galactic winds for understanding the properties of metal absorption systems in the IGM. Among the models they considered, those without galactic feedback could not reproduce the observed evolution of the $\Omega_{\text{C IV}}(z)$, while momentum-driven wind simulations gave the best match with observations, in agreement with the proposal by Oppenheimer & Davé (2006). Similarly, Cen & Chisari (2010) concluded that the dominant mechanism responsible for the metal enrichment of the IGM is star formation feedback from the analysis of

hydrodynamical simulations tuned to reproduce the star formation history of the universe from $z = 6$ to $z = 0$. In these simulations, C IV and O VI are mostly located in regions with temperature $T \geq 2 \times 10^4$ K that have been swept-up by the shocks produced by galactic-scale winds; absorption systems with column densities $N_{\text{C IV}} = 10^{12} - 10^{14}$ cm $^{-2}$ are associated with galaxies of luminosities $L \lesssim L^*$.

While it is generally agreed that galactic outflows are the most likely mechanism for enriching the IGM, the observational evidence for such outflows has so far been limited mostly to galaxies at $z \lesssim 4$. At higher redshifts, even L^* galaxies are too faint to record individual spectral features – other than the Ly α emission line – with sufficient precision to measure kinematic offsets between the stars and the outflowing gas in individual galaxies. Vanzella et al. (2009) did find such offsets in *stacked* spectra of $z = 5$ and 6 galaxies selected from the Great Observatories Origins Deep Survey and indeed concluded that: “powerful, large-scale winds are common at high redshift”. Nevertheless, it is of great interest to explore the outflow phenomenon in more detail at the highest redshifts, as it holds the key not only to the initial stages of the chemical evolution of the Universe, but also presumably to the escape of Lyman continuum photons responsible for reionizing the IGM at $z > 6$.

If the general picture assembled from the above cosmological simulations is correct, most C IV absorption systems at $z > 5$ should be on their first outward trajectory and should be found close to the parent galaxy (Oppenheimer, Davé & Finlator 2009). Then, a key observational test of these models is to identify the star-forming galaxies close to known C IV absorption systems in the spectra of the highest redshifts QSOs.

One of the strongest C IV absorbers in the high- z surveys by Ryan-Weber et al. (2009) and Simcoe et al. (2011) is at $z_{\text{abs}} = 5.7238$ towards the $z_{\text{em}} = 6.309$ QSO SDSS J1030+0524, with rest frame equivalent widths $W_0(\lambda 1548) = 0.65$ Å and $W_0(\lambda 1550) = 0.41$ Å (Ryan-Weber et al. 2009). The field of this QSO was imaged in the i_{775} and z_{850} bands with the Advanced Camera for Surveys (ACS) on the *Hubble Space Telescope (HST)* by Stiavelli et al. (2005). These authors reported a statistical excess of galaxies photometrically classified as *i*-dropouts (i.e. with $i_{775} - z_{850} > 1.3$), and hence potentially located at $z \gtrsim 5.5$. This result was later confirmed by Kim et al. (2009) as part of a larger study of *i*-dropouts around five QSOs at $z \sim 6$. In the latter work, 14 ± 4 *i*-dropouts were found in the field of the QSO SDSS J1030+0524 (~ 11.3 arcmin 2) compared to 8 ± 3 expected from a random distribution of galaxies at these redshifts (Giavalisco et al. 2004). In the absence of spectroscopic redshifts for all but one of the *i*-dropouts – a Ly α emitter at $z = 5.970$, both Stiavelli et al. (2005) and Kim et al. (2009) speculated that the excess galaxies may be part of the same overdensity that includes the QSO.

However, it may also be the case that some of the candidate galaxies are in fact associated with the foreground C IV absorber, particularly as two of the *i*-dropouts lie within ~ 15.5 arcsec of the QSO. This separation corresponds to a transverse distance of ~ 90 kpc (physical) from the QSO line-of-sight at $z = 5.7$; at $z = 2-3$ this is the impact parameter within which strong C IV absorption is found to be associated with actively star-forming galaxies (Steidel et al. 2010). Thus, this field is an ideal location for testing whether

galactic outflows are indeed responsible for producing CIV absorbers at $z > 5.5$, and how the properties of such outflows compare with those at lower redshifts.

Motivated by these considerations, we have performed deep spectroscopic observations of the two galaxies closest to the sight-line to the QSO SDSS J1030+0524, and of the additional galaxy already known to be a Ly α emitter from the discovery paper by Stiavelli et al. (2005). This paper is organised as follows. In Section 2 we describe our spectroscopic observations as well as our reassessment of the photometry of the ACS images obtained by Stiavelli et al. (2005). We present our results in Section 3 and discuss their implications in Section 4. We summarise our conclusions in Section 5. Throughout this work we use AB magnitudes and assume a flat universe with $H_0 = 70 \text{ km s}^{-1} \text{ Mpc}^{-1}$, $\Omega_m = 0.3$ and $\Omega_\lambda = 0.7$.

2 OBSERVATIONS AND DATA REDUCTION

2.1 Spectroscopic Observations

We obtained medium resolution spectra of three galaxies in the field of the QSO SDSS J1030+0524 photometrically identified by Stiavelli et al. (2005) to be at $z > 5.5$. Two of the galaxies were selected as being closest to the QSO sight-line, at transverse distances of $\sim 90 \text{ kpc}$ (assuming that they are at $z = 5.5\text{--}6$). The third galaxy, J103024.08+052420.4, is the only object in the field for which Stiavelli et al. (2005) were able to measure a spectroscopic redshift, $z = 5.970$; we re-observed this source for comparison purposes.

The spectra were obtained with FORS2 on UT1 of the ESO VLT, operated in multi-object spectroscopic mode using $0.7''$ slits with the GRIS_600z grism which covers the wavelength range from 7370 to 11000 \AA . The resolution is $\text{FWHM} = 4.9 \text{ \AA}$ (or 172.5 km s^{-1} at 8500 \AA), sampled with three pixels. A total of 36 exposures of 900 s each were acquired between 2007 April 24 and 2007 June 17; two of these were of very low signal-to-noise ratio and were excluded from the final stack of combined spectra. The total integration time of the final image was 30 600 s.

The observations were carried out in service mode and processed by ESO using automatic pipelines. The data products consist of a sky-subtracted 2D image for each 900 s exposure, wavelength calibrated and corrected for bias, overscan, dark current and flat field. Given the challenging nature of these faint object observations, we also processed the images independently of the ESO pipeline (starting from the sky subtraction stage), using conventional IRAF tasks. Specifically, we combined the two-dimensional slit image of each object with IMCOMBINE and we found a single emission line centered along the spatial axis (slit direction) at the position where each object is expected to be. Then, we extracted individual exposures with APALL and combined them in observational blocks of three exposures with SCOMBINE prior to the flux calibration. Once each block was flux calibrated (using the provided spectroscopic standard star spectra and IRAF tasks STANDARD, SENSFUNC and CALIBRATE), we averaged all the blocks and confirmed the presence of an emission line uncontaminated by sky residuals in the final combined spectrum of each object.

Having performed this independent check, and taking

into consideration that the ESO pipeline was developed specifically to reduce any systematic effect from the telescope and the instrument, we resumed the reduction process of ESO pipeline output files using IRAF. Given that the galaxies are very faint, the sky subtraction residuals in each slit were removed with the task BACKGROUND, using a first order polynomial, before the extraction of individual spectra. Automatic cosmic ray cleaning was carried out at this stage, with a few cosmic-ray affected pixels requiring manual cleaning. Finally, after flux calibrating each spectrum, we combined the spectra of each galaxy in a weighted average, where the weight is the median flux value of the 8–10 pixels centred on the Ly α emission line, which is the only spectral feature detected. The results of our spectroscopic analysis are presented in Section 3.

2.2 Photometry

The existence of an overdensity of galaxies at $z > 5.5$ in the field of the $z = 6.309$ QSO SDSS J1030+0524 first reported by Stiavelli et al. (2005) has more recently been confirmed by Kim et al. (2009). This was not unexpected, given that both studies used the same ACS/HST images, the same colour selection criterion and the same S/N limit. It is therefore somewhat surprising that two out of the three galaxies we targeted, originally communicated to us by M. Stiavelli, [in Stiavelli et al. (2005) no information was provided on individual galaxy positions, magnitudes and colours], are not included in the later compilation by Kim et al. (2009). Having confirmed spectroscopically that both objects are indeed at $z > 5.5$ (at $z = 5.676$ and $z = 5.719$ respectively; see Section 3), we decided to remeasure ourselves the magnitudes z_{850} and colours $i_{775} - z_{850}$ of all three galaxies considered here.

The data retrieved from the public HST archive¹ consist of seven images in the i_{775} band with a total exposure time of 5840 s, and nine images in the z_{850} band with a total exposure time of 11 300 s. We ran MULTIDRIZZLE on the reduced images (*flt* files) with a linear size of output pixels in arcseconds per pixel of $pixscale = 0.6$. The size of a pixel in units of the input pixel size was $pixfrac = 1.0$ and inverse-variance maps were used as weighting image (*final_wght_type = ivm*). Distortion corrections were computed with the most updated distortion coefficient tables available from the Multitemission Archive at the Space Telescope (MAST).

We used SEXTRACTOR version 2.5.0 to calculate the magnitudes and colours of the three galaxies in our sample in order to have a consistent comparison with previous works in the same field. Photometry was performed in pseudo-dual image mode in the z_{850} band and dual image mode in the i_{775} band with the z_{850} as detection image. The weight map from MULTIDRIZZLE was used in the detection image and the corresponding exposure time map was used in the measurement images. We adopted MAG_AUTO as the total magnitude of each source. Zero-point magnitudes were obtained from the Space Telescope Science Institute website² updated on May 19th, 2009. The values corresponding to F775W and F850LP filters for the date of observation

¹ <http://archive.stsci.edu>

² <http://www.stsci.edu/hst/acs/analysis/zeropoints>

are 25.67849 and 26.86663 respectively. Regarding extinction correction, the same values determined by Kim et al. (2009) were used: 0.048 and 0.036 for the i_{775} and z_{850} magnitudes respectively. Colours give in Table 1 were computed using isophotal photometry (MAG_ISO).

Owing to correlated noise introduced by MULTIDRIZZLE in the final image, the errors in magnitude and flux determination provided by SEXTRACTOR are incorrect. To overcome this problem, the first step is to calculate the following correction factor, A , valid in the case $\text{pixscale} (s) \leq \text{pixfrac} (p)$

$$A = \left(\frac{s}{p} - \frac{s^2}{3p^2} \right)^2.$$

Then, we applied the following correction to the error in the flux estimation and the error in the magnitude

$$f_{\text{err}}^c = \sqrt{\frac{f_{\text{err}}^2}{A} - \frac{f}{g \cdot A} + \frac{f}{g}}$$

$$\text{MAG}_{\text{err}}^c = \frac{f_{\text{err}}^c}{f} * \frac{2.5}{\ln(10)},$$

where f_{err} is the flux error estimated by SEXTRACTOR, f is the measured flux and g is the gain.

In Table 1 we list the magnitudes and colours of the three galaxies corrected for correlated noise and galactic extinction. For the one galaxy in common with Kim et al. (2009), J103024.08+052420.41, we find $z_{850} = 25.94 \pm 0.05$ and $i_{775} - z_{850} = 2.25$; for comparison Kim et al. (2009) reported $z_{850} = 25.74$ and $i_{775} - z_{850} = 2.12$ (object A13 in their Table 3).

3 RESULTS

3.1 Lyman alpha detections

As shown in Figs. 1, 2, and 3, we detect a single emission line in each of the three galaxies observed. We interpret these features as Ly α emission lines at redshifts $z_{\text{em}} = 5.7\text{--}6.0$, for the following reasons.

As discussed in more detail below (Section 3.3), the $(i_{775} - z_{850})$ colours of the galaxies together with their faint z_{850} magnitudes are indicative of high redshifts, $z > 5.4$. The main contaminants in this colour regime are galaxies at $z = 1\text{--}2$; in this case, the emission lines we have detected could conceivably be [O II] $\lambda\lambda 3726, 3729$. at $z_{\text{em}} = 1.2\text{--}1.3$. However, the [O II] doublet, with a wavelength separation of $2.8 \times (1 + z) \simeq 6.2 \text{ \AA}$ should be resolved in our spectra, which have a resolution of 4.9 \AA FWHM. Furthermore, even if the individual doublet lines were not fully resolved, we expect the width of the features to be FWHM $\gtrsim 8 \text{ \AA}$, broader than FWHM $\simeq 4.9$ and 6.0 \AA we measure for the two newly discovered emission lines reported here, in Targets 2 and 3 respectively. The emission line in Target 1 was independently identified as Ly α by Stiavelli et al. (2005) on the basis of its asymmetric profile which is characteristic of resonantly scattered Ly α emission in galaxies undergoing large-scale outflows (e.g. Quider et al. 2009). We conclude that the most likely interpretation is that all three features are Ly α emission lines at redshifts $z_{\text{em}} = 5.7\text{--}6.0$, as detailed below.

We measured the values of z_{em} for each galaxy from the peak of the emission line; we estimate the uncertainty of

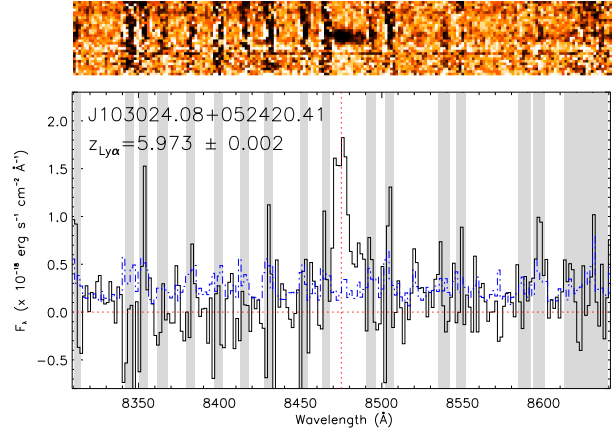


Figure 1. FORS2 spectrum of J103024.08+052420.41. Top: 2D image of the spectrum. The x -axis is wavelength and the y -axis is the spatial direction along the slit. Bottom: 1D spectrum, with the dotted line showing the 1σ error spectrum. Grey regions indicate positions of all the sky lines present (with different intensities). In both 2D and 1D spectra, an emission line is clearly detected at 8477 \AA ; we identify this feature as Ly α at $z = 5.973$.

the redshifts to be ± 0.002 from consideration of the seeing and spectral resolution of our data. However, it should be borne in mind that the Ly α forest could absorb a significant fraction of the emission on the blue wing of the line, leading to an overestimate of the redshift.

We also measured the line flux, from which we calculate $L_{\text{Ly}\alpha}$, the Ly α luminosity in our cosmology. This in turn can be used to estimate the star formation rate, $\text{SFR}_{\text{Ly}\alpha}$, using Kennicutt’s (1998) calibration of $\text{SFR}_{\text{H}\alpha}$ and case B recombination

$$\text{SFR}_{\text{Ly}\alpha} (\text{M}_{\odot} \text{yr}^{-1}) = 9.1 \times 10^{-43} L_{\text{Ly}\alpha} (\text{ergs}^{-1}). \quad (1)$$

The above conversion assumes a standard Salpeter (1955) stellar initial mass function (IMF); adopting the Chabrier (2003) IMF which has proportionally fewer low mass stars would reduce the values of $\text{SFR}_{\text{Ly}\alpha}$ by a factor of ~ 1.8 . On the other hand, it is well known that the uncorrected Ly α emission line luminosity can lead to significant *underestimates* of the SFR – not only because of overlapping absorption by the Ly α forest, but especially as a consequence of resonant scattering. Multiply scattered Ly α photons can be absorbed by even small quantities of dust and can diffuse spatially over extended halos greater than the projected size of the spectrograph slit (Steidel et al. 2011). We now briefly discuss each galaxy in turn.

3.1.1 Target 1: J103024.08+052420.41

This is the only galaxy with spectroscopic confirmation in the sample of Stiavelli et al. (2005). We detect a clear ($\sim 15\sigma$) emission line (see Fig. 1) which we identify as Ly α at $z_{\text{Ly}\alpha} = 5.973 \pm 0.002$, in good agreement with the redshift $z_{\text{Ly}\alpha} = 5.970$ reported by Stiavelli et al. (2005). The total line flux is $F_{\text{Ly}\alpha} = 22 \pm 1.5 \times 10^{-18} \text{ erg s}^{-1} \text{ cm}^{-2}$, measured by integrating over $\sim 23 \text{ \AA}$ ($\sim 800 \text{ km s}^{-1}$) of the spectrum; it is not possible to compare with the data by Stiavelli et al. (2005) because these authors did not report a measurement

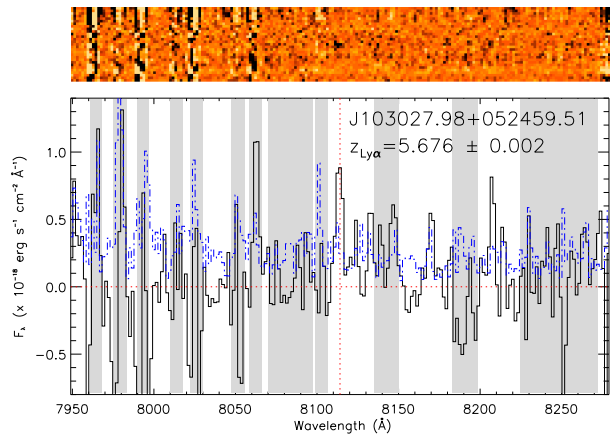


Figure 2. FORS2 spectrum of J103027.98+052459.51. Details as in Figure 1.

of the line flux. The Ly α line flux corresponds to a luminosity $L_{\text{Ly}\alpha} = 8.6 \pm 0.6 \times 10^{42} \text{ erg s}^{-1}$ in our cosmology, and a star formation rate $\text{SFR}_{\text{Ly}\alpha} = 7.8 \pm 0.5 M_{\odot} \text{ yr}^{-1}$ with the conversion (and caveats) given above (see Table 1).

3.1.2 Target 2: J103027.98+052459.51

As can be seen from Fig. 2, we detect a weak and narrow emission line which we interpret as Ly α emission at $z = 5.676 \pm 0.002$. With a line flux $F_{\text{Ly}\alpha} = 4.9 \pm 1.1 \times 10^{-18} \text{ erg s}^{-1} \text{ cm}^{-2}$, the detection is significant at the $\sim 4.5\sigma$ level. Although the line is weak, it does fall in a relatively clean region of the spectrum, free from obvious residuals from the subtraction of sky emission lines (see top panel of Fig. 2). The corresponding luminosity and star formation rate are, respectively, $L_{\text{Ly}\alpha} = 1.7 \pm 0.4 \times 10^{42} \text{ erg s}^{-1}$ and $\text{SFR}_{\text{Ly}\alpha} = 1.6 \pm 0.4 M_{\odot} \text{ yr}^{-1}$ (see Table 1). The line has $\text{FWHM} \simeq 150 \text{ km s}^{-1}$ after correcting for the instrumental resolution. Although this galaxy is relatively close to the QSO sight-line, at a projected distance of 83 kpc, no C IV absorption at its redshift was reported by either Ryan-Weber, Pettini & Madau (2006) nor Simcoe et al. (2011).

3.1.3 Target 3: J103026.49+052505.14

At a projected distance of 79 kpc, this galaxy is the closest to the QSO sight-line among the three galaxies targeted by our observations. We detect a weak emission line centred at $\lambda_{\text{obs}} = 8168 \text{ \AA}$, in a clean region of the spectrum, free from strong sky line residuals (see Fig. 3). We identify the feature as Ly α emission at $z = 5.719 \pm 0.002$, with a flux $F_{\text{Ly}\alpha} = 4.3 \pm 0.9 \times 10^{-18} \text{ erg s}^{-1} \text{ cm}^{-2}$ ($\sim 4.8\sigma$ level detection). This corresponds to a luminosity $L_{\text{Ly}\alpha} = 1.5 \pm 0.3 \times 10^{42} \text{ erg s}^{-1}$ and star formation rate $\text{SFR}_{\text{Ly}\alpha} = 1.4 \pm 0.3 M_{\odot} \text{ yr}^{-1}$.

The emission line redshift differs by $\Delta v = -214 \text{ km s}^{-1}$ from the redshift $z_{\text{abs}} = 5.7238 \pm 0.0001$ of the strongest C IV absorption system in the spectrum of the QSO, with column density $N_{\text{C IV}} = 2.3 \times 10^{14} \text{ cm}^{-2}$ (Ryan-Weber, Pettini & Madau 2006). More recently, Simcoe et al. (2011) reported $z_{\text{abs}} = 5.72438$, corresponding to $\Delta v = -240 \text{ km s}^{-1}$, and $N_{\text{C IV}} = 3.9 \times 10^{14} \text{ cm}^{-2}$ for this

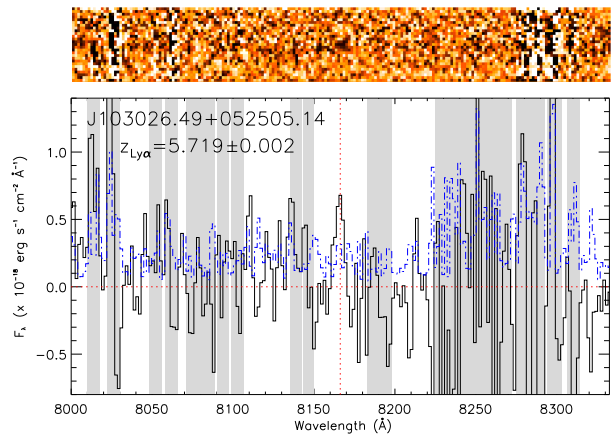


Figure 3. FORS2 spectrum of J103026.49+052505.14. Details as in Figure 1.

absorber, measured from near-IR spectra obtained with the Folded Port Infrared Echellette (FIRE) instrument on the 6.5 m Magellan telescope.

The velocity difference between the Ly α emission line and the C IV system may be due to random error ($\sim 2-3\sigma$) and/or systematic errors in the wavelength scale of either the FORS2 spectrum reported here or the near-IR spectra analysed by Ryan-Weber, Pettini & Madau (2006) and Simcoe et al. (2011). Alternatively, it may be an indication that the geometry of the outflowing (or perhaps inflowing) gas associated with this galaxy is not spherically symmetric. The velocity offset could be larger if the Ly α emission line is redshifted relatively to the systemic redshift of the galaxy, as is normally the case in galaxies driving large scale outflows (e.g. Pettini et al. 2001; Steidel et al. 2010). In any case, as we discuss below, this galaxy is sufficiently close to the QSO sight-line for an outflow at the canonical $v_{\text{out}} = 200 \text{ km s}^{-1}$ to have travelled the projected distance of 79 kpc in $\sim 0.4 \text{ Gyr}$, less than half the age of the Universe at $z = 5.7$.

3.2 UV luminosities

In this section we derive the UV continuum fluxes of the galaxies from their z_{850} magnitudes and use them to deduce values of the star formation rate SFR_{UV} for comparison with the values of $\text{SFR}_{\text{Ly}\alpha}$ measured above. At $z = 5.7-6.0$, the z_{850} filter samples the far-UV spectrum where, according to Madau, Pozzetti & Dickinson (1998)

$$L_{\text{UV}}(\text{ergs}^{-1}\text{Hz}^{-1}) = 8.0 \times 10^{-27} \text{SFR}_{\text{UV}}(M_{\odot}\text{yr}^{-1}) \quad (2)$$

for a Salpeter IMF. As mentioned earlier, an IMF with fewer low-mass stars, such as that appropriate to the Milky Way (Chabrier 2003), would lead to lower values of SFR by a factor of ~ 1.8 . The conversion in eq. (2) applies to the UV continuum at 1500 \AA , but the intrinsic (i.e. before reddening) UV slope of starburst galaxies is approximately flat in F_{ν} between 1500 and 1200 \AA , so that the above conversion should still apply. On the other hand, the reddening correction is unknown for our galaxies; thus the values of SFR_{UV} we derive are strictly lower limits. Furthermore, eq. (2) is valid for the ideal case of a continuous star formation

Table 1. Ly α and UV parameters, magnitudes and colours of the targets.

Object	Target 1	Target 2	Target 3
R.A. (J2000)	10 30 24.08	10 30 27.98	10 30 26.49
Dec. (J2000)	+05 24 20.41	+05 24 59.51	+05 25 05.14
z_{850}^a (mag)	25.94 ± 0.05	26.03 ± 0.06	25.34 ± 0.05
$(i_{775} - z_{850})^b$	2.25	1.23	1.59
$z_{Ly\alpha}^c$	5.973 ± 0.002	5.676 ± 0.002	5.719 ± 0.002
$L_{Ly\alpha}$ ($\times 10^{42}$ erg s $^{-1}$)	8.6 ± 0.6	1.7 ± 0.4	1.5 ± 0.3
SFR $_{Ly\alpha}$ (M_{\odot} yr $^{-1}$)	7.8 ± 0.5	1.6 ± 0.4	1.4 ± 0.3
F_{UV}^d ($\times 10^{-30}$ erg s $^{-1}$ cm $^{-2}$ Hz $^{-1}$)	1.13 ± 0.08	1.29 ± 0.08	2.6 ± 0.1
L_{UV} ($\times 10^{28}$ erg s $^{-1}$ Hz $^{-1}$)	6.4 ± 0.4	6.8 ± 0.4	13.6 ± 0.7
SFR $_{UV}$ (M_{\odot} yr $^{-1}$)	8.0 ± 0.5	8.5 ± 0.5	17.0 ± 0.9
Physical distance e (kpc)	326	83	79

^aCalculated using FLUX_AUTO.

^bCalculated using FLUX_ISO.

^cVacuum heliocentric.

^dCorrected for Ly α emission and Ly α forest.

^eTransverse distance to the QSO line-of-sight.

episode lasting for more than 100 Myr; younger ages would lead to larger values SFR $_{UV}$.

Two corrections that we can apply, knowing the wavelengths of the Ly α emission lines and the transmission curve of the ACS F850LP filter, are for absorption by the Ly α forest and for the contribution to the z_{850} magnitudes by the Ly α emission line itself. For the latter, we simply subtracted the flux of the Ly α line from the flux measured by SExtractor in the z_{850} band (FLUX_AUTO). The correction for Ly α forest absorption is a multiplicative factor accounting for the fact that not all the filter was illuminated in wavelength space. We applied the following correction to amend for this effect

$$f_{\nu_0}^{c2} = f_{\nu_0}^c \cdot \frac{A_T}{A_F}$$

where $f_{\nu_0}^c$ is the UV flux corrected for Ly α emission, A_T is the total area under the throughput curve and A_F is the area under the same curve for wavelengths $\lambda > \lambda_{\text{obs}}(\text{Ly}\alpha)$ (thus assuming that, to a first approximation, there is negligible flux below the Ly α emission line).

As can be seen from Table 1, SFR $_{UV} > \text{SFR}_{Ly\alpha}$ for all three galaxies. As mentioned above (Section 3.1), there are many possible reasons which can explain the common finding that the Ly α line luminosity underestimates the true star formation rate in galaxies. It is interesting that, out of the three galaxies observed, it is the one with the clearest evidence for a large-scale outflow (Target 3) that shows the largest difference between SFR $_{UV}$ and SFR $_{Ly\alpha}$. As discussed by Steidel et al. (2011), galaxy-scale outflows naturally lead to a diffuse, extended halo of Ly α emission which is seldom captured in its entirety with slit spectroscopy.

3.3 Color confirmation

Having confirmed that all three targets are indeed at $z = 5.5$ – 6 , we comment briefly on the colour selection for i -dropouts. According to Malhotra et al. (2005), the colour cut $i_{775} - z_{850} > 0.9$ in sources with $z_{850} \leq 27.5$ will include galaxies at $z > 5.4$ with a completeness of $\sim 80\%$. However, galaxies at intermediate redshifts ($z \simeq 1$ – 2) also have $i_{775} - z_{850} \sim 1$. Therefore, a color cut $i_{775} - z_{850} > 1.3$ may

be a stronger criterion for eliminating lower redshift interlopers, but it was noticed by Malhotra et al. (2005) that it would lead to higher incompleteness (~ 20 – 30%) for $z \sim 6$ galaxies.

Concerning our three galaxies, we note that Target 1 has the reddest colour, $i_{775} - z_{850} = 2.25$, but the lowest UV flux, once corrections have been applied for Ly α forest absorption and Ly α emission (see Table 1). The reason is that the Ly α emission line makes a significant contribution to the flux measured in the z_{850} filter.

With $z_{850} = 26.03 \pm 0.06$ Target 2 is the faintest of the three in this band, even though its corrected UV flux is not the lowest. Note that with $i_{775} - z_{850} = 1.23$ this galaxy would be missed by a colour selection $i_{775} - z_{850} > 1.3$, even though it is intrinsically bright: its UV luminosity, $L_{UV} = 6.8 \times 10^{28}$ erg s $^{-1}$ Hz $^{-1}$, corresponds to $L_{UV} = 1.25 L_{z=6}^*$, adopting $L_{z=6}^* = 5.44 \times 10^{28}$ erg s $^{-1}$ Hz $^{-1}$ from Bouwens et al. (2007).

Target 3, which we associate with the C IV absorber at $z = 5.7238$, has the brightest z_{850} magnitude of the three objects ($z_{850} = 25.34 \pm 0.05$ mag) and is also the most luminous with $L_{UV} = 2.5 L_{z=6}^*$. In this case, the weak Ly α line does not make a significant contribution to the integrated flux in the F850LP filter, resulting in a smaller correction to the z_{850} magnitude than for Target 1.

In conclusion, while there is evidence that the colour cut $i_{775} - z_{850} > 1.3$ is effective against low redshift interlopers, our (admittedly limited) results show that it can also miss a significant proportion of luminous ($L > L^*$) galaxies at $z > 5.5$. Possibly, a less extreme colour cut, such as $i_{775} - z_{850} > 1.2$, may be more suitable for galaxies at $z \gtrsim 5.7$ with faint Ly α emission.

4 DISCUSSION

4.1 Connection between star forming galaxies and C IV absorption systems

To recap, in order to investigate the origin of C IV absorbers at $z \sim 6$, we have examined the field of the QSO SDSS J1030+0524, whose spectrum shows the strongest C IV ab-

sorption doublet in the survey by Ryan-Weber et al. (2009), and discovered two Ly α emitters at $z \simeq 5.7$ close to the QSO sight-line (and confirmed a previously known Ly α emitter at $z \sim 5.97$). The redshift of J103026.49+052505.14 (Target 3), which is the galaxy closest to the QSO and the most luminous of the three, differs by only $\Delta v \simeq -230 \text{ km s}^{-1}$ from that of the C IV absorption lines³; this finding is highly suggestive of an association between galaxy and QSO absorber.

At lower redshifts ($z = 2\text{--}3$), the galaxy-QSO absorber connection has now been quantified in some detail (e.g. Adelberger et al. 2003, 2005; Crighton et al. 2010; Steidel et al. 2010). In the last of these studies in particular, the authors derived a rough relationship between the equivalent width of the stronger member of the C IV doublet, $W_0(\lambda 1548)$, and the projected distance between the galaxy and the QSO sight-line (see Fig. 21 of Steidel et al. 2010). It is thus of interest to verify whether this relationship also holds at much higher redshifts, at least in the case of J103026.49+052505.14.

The first point to note is that, with a $\text{SFR}_{\text{UV}} = 17.0 M_{\odot} \text{ yr}^{-1}$, J103026.49+052505.14 is typical of the galaxies driving outflows at redshifts $z = 2\text{--}3$ in the sample of Steidel et al. (2010). Second, the rest-frame equivalent width of C IV $\lambda 1548$ at $z_{\text{abs}} = 5.7238$ in the spectrum of SDSS J1030+0524 is $W_0(\lambda 1548) = 0.65 \text{ \AA}$ (Ryan-Weber et al. 2009). This value is intermediate between the last two points in the $W_0(\lambda 1548)$ vs. galactocentric impact parameter b plot constructed by Steidel et al. (2010), between which the line equivalent width drops dramatically from $W_0(\lambda 1548) = 1.2 \pm 0.15 \text{ \AA}$ at $b = 63 \text{ kpc}$ to $W_0(\lambda 1548) = 0.13 \pm 0.05 \text{ \AA}$ at $b = 103 \text{ kpc}$. If we simply interpolate between these two points, we find that $W_0(\lambda 1548) = 0.65 \text{ \AA}$ is *on average* expected to be measured at impact parameters $b \simeq 70 \text{ kpc}$. For comparison, the 13.5 arcsec separation on the sky between the galaxy J103026.49+052505.14 and the QSO SDSS J1030+0524 corresponds to an impact parameter $b = 79 \text{ kpc}$ at $z_{\text{abs}} = 5.7238$. Given the uncertainties in the interpolation and the likely spread of the average relationship between $W_0(\lambda 1548)$ and b when applied to any individual galaxy, we conclude that the strength of the C IV absorption seen 79 kpc from the galaxy J103026.49+052505.14 is typical of the galaxy-scale outflows operating at redshifts $z = 2\text{--}3$.

4.2 Outflow Speed

With only the Ly α line at our disposal, we do not have any information on the speed of the outflow from J103026.49+052505.14 which has spread metals over radii of at least 79 kpc. Furthermore, in the absence of the IR photometry necessary to characterise the spectral energy distribution of this galaxy, we have no means to estimate the age of the starburst. Nevertheless, it is instructive to consider some relevant timescales.

The analysis by Steidel et al. (2010), together with the results of high resolution spectroscopy of gravitationally lensed star-forming galaxies at $z = 2\text{--}3$ (e.g. Pettini et al.

2002; Quider et al. 2009; Dessauges-Zavadsky et al. 2010, and references therein), has shown that while galactic winds may be launched with speed of typically $\sim 200 \text{ km s}^{-1}$, the gas accelerates outwards reaching speeds of up to 800 km s^{-1} before reaching the virial radius. If the bulk of the gas outflowing from J103026.49+052505.14 were indeed moving at $v_{\text{out}} = 800 \text{ km s}^{-1}$, it would reach distances of $\sim 80 \text{ kpc}$ – and could produce absorption in the QSO spectrum – in only $\sim 100 \text{ Myr}$.

On the other hand, other authors have considered more modest outflow velocities, largely on theoretical grounds. Martin et al. (2010) argued that average outflow speeds of less than 200 km s^{-1} are required to match the line-of-sight correlation function of C IV absorbers at redshifts $z = 1.7\text{--}4.5$. Oppenheimer & Davé (2006) favour such velocities because in their cosmological simulations they are found to be sufficiently high to enrich the low density IGM and yet low enough to avoid overheating it. More recently, Kramer, Haiman & Madau (2010) pointed out that the rapid rise in the intergalactic density of C IV from $z = 5.8$ and 4.7 discovered by Ryan-Weber et al. (2009) and Becker, Rauch & Sargent (2009) may be inconsistent with the near-complete reionization of the IGM by $z \simeq 6$ and the slower build-up of stellar mass during this epoch. All of these observations can be reconciled, however, if there is a delay of $\sim 400\text{--}700 \text{ Myr}$ between the onset of star formation and the appearance of its products (i.e. the metals) at distances of $\sim 100 \text{ kpc}$ from the sites of productions. The corresponding outflow speeds implied by this argument are also of order $\sim 200 \text{ km s}^{-1}$.

Adopting a more modest value $v_{\text{out}} = 200 \text{ km s}^{-1}$ for the outflow from J103026.49+052505.14 would imply a travel time $t \sim 400 \text{ Myr}$ to reach the QSO sight-line. In turn, this would place the onset of star formation in this galaxy at $z = 8.4$ where galaxies are now claimed to be found in increasing numbers (e.g. Bouwens et al. 2010, 2011). In future, deep observations of this and other galaxies in the field of the QSO SDSS J1030+0524 at infrared wavelengths should allow a rough determination of the age of the galaxy from which an estimate of the speed of the outflows may be inferred.

4.3 Contribution to the IGM

Steidel et al. (2010) showed that, given the typical extent ($\approx 90 \text{ kpc}$) of metal-enriched regions around star-forming galaxies at $z \sim 2$, galaxies brighter than $\sim 0.3L^*$ can account for approximately half of the number of C IV absorption systems with $W_0(\lambda 1548) \geq 0.15 \text{ \AA}$ seen in QSO spectra at this average redshift. The corollary of this statement is that a galaxy with $L \gtrsim 0.3L^*$ should be found within $\approx 90 \text{ kpc}$ of half the QSO absorbers, with the remainder presumably associated with fainter galaxies.

Given that the properties of the outflow from J103026.49+052505.14 are at least superficially similar to those of star-forming galaxies at $z = 2\text{--}3$, as discussed above, we can repeat the same exercise at the higher redshifts considered here. Specifically, we estimate the number of C IV absorption systems per unit of redshift $(dN/dz)_{\text{CIV,pred}}$ expected from galaxies detected in the field of QSO SDSS J1030+0524 at $z \sim 5.7$, using the model proposed by Steidel et al. (2010). Through a comparison with the ob-

³ Averaging the values of Δv implied by the measurements of z_{abs} (C IV) reported by Ryan-Weber, Pettini & Madau (2006) and Simcoe et al. (2011)—see Section 3.1.3.

served value of $dN/dz(\text{CIV})$, we draw conclusions on the properties of galaxies contributing to the metal enrichment of the IGM at $z \sim 6$ and calculate the chances that the $z_{\text{abs}} = 5.7238$ C IV system may be produced by an undetected, fainter, galaxy instead of J103026.49+052505.14.

We consider the limiting magnitude in the ACS images to estimate an upper limit to the UV luminosity of undetected galaxies. Adopting the $z \sim 6$ luminosity function by Bouwens et al. (2007) ($M_{\text{UV}}^* = -20.24 \pm 0.19$, $\phi^* = 1.4_{-0.4}^{+0.6} \times 10^{-3} \text{ Mpc}^{-3}$, $\alpha = -1.74 \pm 0.16$) we find that the ACS images of the field are sufficiently deep to reveal galaxies with luminosity $L \gtrsim 0.9 L_{z=6}^*$. Integrating the luminosity function, we find that the number density of galaxies with $L \gtrsim 0.9 L_{z=6}^*$ is $n_{\text{gal}} \simeq 0.287 \times 10^{-3} h^3 \text{ Mpc}^{-3}$. If the model by Steidel et al. (2010) is still valid at $z \geq 5.5$, the co-moving cross section for absorption per galaxy is $\sigma_{\text{gal}} \simeq 1.15 \text{ Mpc}^2$ for an impact parameter $b \simeq 90 \text{ kpc}$ (physical). At the $z_{\text{abs}} = 5.7238$ of the C IV absorber, the comoving pathlength per unit of redshift is $dl/dz \simeq 448 \text{ Mpc}$.

Thus, we want to know the predicted number of absorption systems per unit of redshift

$$\frac{dN}{dz}(\text{CIV})_{\text{pred}} = n_{\text{gal}} \sigma_{\text{gal}} \frac{dl}{dz}$$

with $W_0(\lambda 1548) \geq 0.15 \text{ \AA}$. With the above values for n_{gal} , σ_{gal} and dl/dz , we find $dN/dz(\text{CIV})_{\text{pred}} \simeq 0.15$. This estimate is $\approx 30\%$ of the observed value $dN/dz(\text{CIV})_{\text{obs}} = 0.5 \pm 0.3$ at redshift $\langle z \rangle = 5.75$ estimated by Oppenheimer, Davé & Finlator (2009), from the results of Ryan-Weber et al. (2009), and Becker, Rauch & Sargent (2009) for absorption systems with column densities in the range $\log N_{\text{CIV}} = 14.0\text{--}15.0 \text{ cm}^{-2}$. The shortfall is presumably higher when we include weaker C IV systems, since the Steidel et al. (2010) limit $W_0(\lambda 1548) \geq 0.15$ corresponds to column densities $\log N_{\text{CIV}} \geq 13.6 \text{ cm}^{-2}$ for unsaturated absorption lines, somewhat lower than the column density of C IV for which absorption line statistics are currently available at these high redshifts.

We conclude that, if star-forming galaxies at $z \sim 5.7$ have enriched surrounding regions to radii of $\sim 90 \text{ kpc}$, as is the case at $z = 2\text{--}3$, it is necessary to reach at least $L_{\text{UV}} \sim 0.4 L_{z=6}^*$ ($M_{\text{UV}}^* \sim -19.24$, i.e. one magnitude fainter than the ACS images considered in this work) in order to detect the full population of galaxies linked to absorption systems with $\log N_{\text{CIV}} = 14.0\text{--}15.0 \text{ cm}^{-2}$.

5 CONCLUSIONS

From deep spectroscopy of galaxies in the field of $z_{\text{em}} = 6.309$ QSO SDSS J1030+0524 we have identified three Ly α emitters at $z \geq 5.7$. Of these three galaxies, the brightest ($L_{\text{UV}} = 2.5 L_{z=6}^*$) and closest to the QSO sight-line (impact parameter $b = 79 \text{ kpc}$), J103026.49+052505.14, is at a redshift $z = 5.719$ which differs by only $\Delta v \simeq -230 \text{ km s}^{-1}$ from the absorption redshift of a strong C IV system in the spectrum of the QSO.

The chances of a random association between Ly α emitter and C IV absorber are very low. For example, if we first consider the idealised case of a random distribution of galaxies with $n_{\text{gal}} \simeq 1.23 \times 10^{-3} \text{ Mpc}^{-3}$, appropriate to galaxies of luminosity $L \gtrsim 0.4 L_{z=6}^*$, then there is only a 1.1×10^{-3}

($\sim 0.1\%$) chance of finding such a galaxy within a sphere of radius 90 kpc (physical) centred on the QSO sight-line at $z = 5.7238$. However, for this calculation it is more appropriate to consider a cylinder, rather than a sphere, with radius 90 kpc but depth along the line of sight corresponding to $\Delta v \simeq \pm 230 \text{ km s}^{-1}$, the velocity difference between the Ly α emitter and the C IV absorber. The volume of this configuration is approximately six times larger than that of a sphere of radius 90 kpc , raising the probability of finding a galaxy by chance within this volume to $\sim 0.7\%$.

A second factor to take into account is galaxy clustering. Indeed, Stiavelli et al. (2005) and Kim et al. (2009) reported an overdensity by a factor of ~ 2 at $z > 5.5$ in the field of the QSO J1030+0524. If this average factor applied to the environment of the galaxy J103026.49+052505.14, the above probability would be increased by a factor of two. More important, however, is the possibility of significant clustering with lower luminosity dwarf galaxies which would remain unrecognised given the current limits of the photometry in this field. Extending the above calculations further down the luminosity function, to galaxies as faint as $\sim 0.06 L_{z=6}^*$, would increase the above probability by one order of magnitude. Indeed, the $\sim 230 \text{ km s}^{-1}$ velocity difference between Ly α emission and C IV absorption could be taken as evidence for an origin of the metals in a dwarf galaxy in the same overdensity as J103026.49+052505.14. On the other hand, at present we have no way of addressing empirically the question of whether such low-luminosity galaxies support large-scale outflows of metal-enriched gas, and how their mass-outflow rates compare with those of the more luminous galaxies in which the outflows are seen directly.

The result reported here is the first direct observational evidence that the circum-galactic medium of early luminous star-forming galaxies was already enriched with heavy elements at $z \sim 6$. Even at these high redshifts, some of the properties of the galaxy-wide outflows responsible for enriching the circum-galactic medium appear to be superficially similar to those of their counterparts at $z = 2\text{--}3$, which have been characterised in some detail. In particular, the strength of the C IV absorption associated with J103026.49+052505.14 at a radial distance of 79 kpc fits in well with expectations based on data appropriate to lower redshifts galaxies, even though the average density of the IGM was much higher at $z \sim 6$ than at $z = 2\text{--}3$.

We emphasise the importance of extending the available photometry of J103026.49+052505.14 to include near-IR bands from which the SED of the galaxy can be determined with the accuracy required to deduce its age. With this information in hand, it should be possible to estimate the average speed of the outflow which has transported the metals out to at least $\sim 80 \text{ kpc}$ from the stars that produced them. If a speed $v_{\text{out}} \simeq 200 \text{ km s}^{-1}$ is appropriate, as argued by some, the starburst episode must have lasted at least $\sim 400 \text{ Myr}$, placing its origin at $z \simeq 8.4$; we now know this to have been an epoch when star-formation in galaxies was already underway. Higher outflow speeds would imply later onsets of the starburst.

The observations presented here show that it is feasible, with dedication, to identify the galaxies linked to QSO absorption systems even at the highest redshifts where intervening metals have been detected in QSO spectra, and thus provide an incentive to pursue similar searches in

other fields. Finally, we also point out that the colour cut $i_{775} - z_{850} > 1.3$ which has been proposed to avoid low redshift interlopers can miss a significant proportion of bluer galaxies at $z \gtrsim 5.7$ thus affecting mainly the LAE population. We are pursuing this topic in a forthcoming paper.

ACKNOWLEDGMENTS

We are grateful to Massimo Stiavelli who kindly shared his ACS images of the QSO field in advance of publication, and to Ben Oppenheimer and Masami Ouchi for stimulating discussions. We thank the referee, Neil Crighton, for valuable suggestions that improved the paper. CGD acknowledges financial support by the Victorian State Government through the International Research Scholarship Program; ERW's research is supported by Australian Research Council grant DP1095600; PM acknowledges support by the NSF through grant AST-0908910.

REFERENCES

- Adelberger, K. L., Steidel, C. C., Shapley, A. E., & Pettini, M. 2003, *ApJ*, 584, 45
- Adelberger, K. L., Shapley, A. E., Steidel, C. C., Pettini, M., Erb, D. K. & Reddy, N. A. 2005, *ApJ*, 629, 636
- Becker, G. D., Sargent, W. L. W., Rauch, M. & Simcoe, R. 2006, *ApJ*, 640, 69
- Becker, G. D., Rauch, M. & Sargent, W. L. W. 2009, *ApJ*, 698, 1010
- Becker, G. D., Sargent, W. L. W., Rauch, M., & Calverley, A. P. 2011, *ApJ*, submitted (arXiv:1101.4399)
- Bouwens, R. J., Illingworth, G. D., Franx, M., Ford, H. 2007, *ApJ*, 670, 928
- Bouwens, R. J., et al. 2010, *ApJ*, 709, L133
- Bouwens, R. J., et al. 2011, *ApJ*, in press (arXiv:1006.4360)
- Cen, R., Chisari, N. E. 2011, *ApJ*, 731, 11
- Chabrier, G. 2003, *PASP*, 115, 763
- Crighton, N. H. M., et al. 2010, *MNRAS*, in press (arXiv:1006.4385).
- Davé, R. & Oppenheimer, B. D. 2007, *MNRAS*, 374, 427
- Dessauges-Zavadsky, M., D'Odorico, S., Schaerer, D., Modigliani, A., Tapken, C., & Vernet, J. 2010, *A&A*, 510, A26
- Giavalisco, M., et al. 2004, *ApJ*, 600, L93
- Heckman, T. M., Lehnert, M. D., Strickland, D. K., & Armus, L. 2000, *ApJS*, 129, 493
- Kennicutt, R. C., Jr. 1998, *ARAA*, 36, 189
- Kim, S., et al. 2009, *ApJ*, 695, 809
- Kramer, R., Haiman, Z. & Madau, P. 2010 *astro-ph/arXiv:1007.3581*, submitted to *MNRAS*
- Madau, P., Pozzetti, L. & Dickinson, M. 1998, *ApJ*, 498, 106
- Madau, P., Ferrara, A. & Rees M. J. 2001, *ApJ*, 555, 92
- Malhotra, S., et al. 2005, *ApJ*, 626, 666
- Martin, Crystal L. 2005, *ApJ*, 621, 227
- Martin, C., Scannapieco, E., Ellison, S., Hennawi, J., Djorgovski, S. & Fournier, A. 2010, *ApJ*, 721, 174
- Oppenheimer, B. D. & Davé, R. 2006, *MNRAS*, 373, 1265
- Oppenheimer, B. D., Davé, R. & Finlator, K. 2009, *MNRAS*, 396, 729
- Oppenheimer, B. D. & Davé, R. 2008, *MNRAS*, 387, 577
- Oppenheimer, B. D. & Davé, R. 2008, *MNRAS*, in press
- Pettini, M., Shapley, A. E., Steidel, C. C., Cuby, J.-G., Dickinson, M., Moorwood, A. F. M., Adelberger, K. L., & Giavalisco, M. 2001, *ApJ*, 554, 981
- Pettini, M., Rix, S. A., Steidel, C. C., Adelberger, K. L., Hunt, M. P., & Shapley, A. E. 2002, *ApJ*, 569, 742
- Pettini, M., Madau, P., Bolte, M., Prochaska, J. X., Ellison, S. L. & Fan, X. 2003, *ApJ*, 594, 695
- Porciani, C. & Madau, P. 2005, *ApJ*, 625, L43
- Powell, L., Slyz, A. & Devriendt, J. 2010 *astro-ph/arXiv:1012.2839*, submitted to *MNRAS*
- Quider, A. M., Pettini, M., Shapley, A. E., & Steidel, C. C. 2009, *MNRAS*, 398, 1263
- Rupke, D. S., Veilleux, S. & Sanders, D. B. 2005, *ApJS*, 160, 115
- Ryan-Weber, E. V., Pettini, M. & Madau, P. 2006, *MNRAS*, 371, 78
- Ryan-Weber, E. V., Pettini, M., Madau, P. & Zych, B. J. 2009, *MNRAS*, 395, 1476
- Salpeter, E. E. 1955, *ApJ*, 121, 161
- Shapley, A. E., Steidel, C. C., Pettini, M., & Adelberger, K. L. 2003, *ApJ*, 588, 65
- Simcoe R. A. 2006, *ApJ*, 653, 977
- Simcoe R. A. 2011, *ApJ*, in press
- Simcoe R. A., et al. 2011, *ApJ*, in press
- Songaila, A. 2001, *ApJ*, 561, L153
- Steidel, C. C., Adelberger, K. L., Shapley, A. E., Erb, D. K., Reddy, N. A. & Pettini, M. 2005, *ApJ*, 626, 44
- Steidel, C. C., Erb, D. K., Shapley, A. E., Pettini, M., Reddy, N., Bogosavljević, M., Rudie, G. C. & Rakic, O. 2010, *ApJ*, 717, 289
- Steidel, C. C., Bogosavljević, M., Shapley, A. E., Kollmeier, J. A., Reddy, N. A., Erb, D. K., & Pettini, M. 2011, *ApJ*, in press (arXiv:1101.2204)
- Stiavelli, M., et al. 2005, *ApJ*, 622, L1
- Tescari, E., Viel, M., D'Odorico, V., Cristiani, S., Calura, F., Borgani, S., Tornatore, L. 2011, *MNRAS*, 411, 826
- Vanzella, E., et al. 2009, *ApJ*, 695, 1163
- Weiner, B. J., et al. 2009, *ApJ*, 692, 187